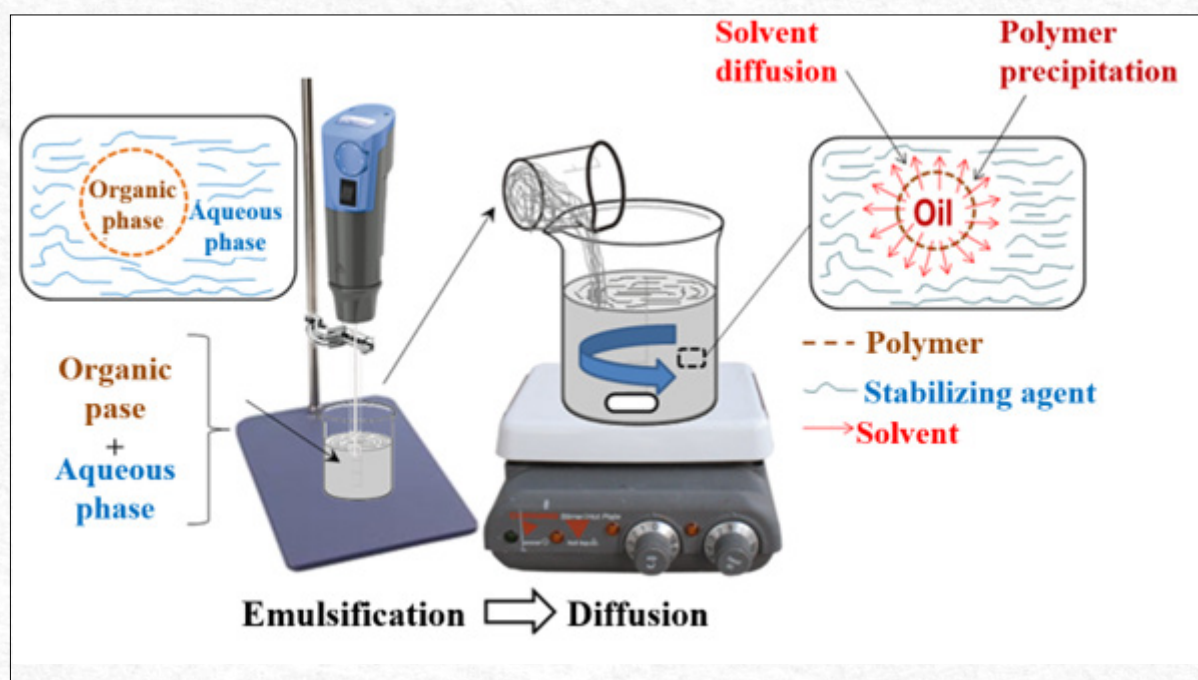


Encapsulation and controlled release of 1,4-naphthoquinone in PDLA nanoparticles: design, biological efficacy, and cancer targeting

K.González^{1,2*}; E.Del Carpio^{2*}; G.González^{3,4};
M.L.Serrano²; J.V.L. Da Silva⁵; M.A. Sabino^{5,6}

*Corresponding author: E-mail address: karina.gonzalez@ucv.ve; *edgar.delcarpio@ucv.ve

Received: October 2024; Accepted: December 2024.



Abstract: Drug release can be controlled by encapsulating active compounds in polymeric vehicles. Using nanotechnology, pharmaceutical drug delivery systems can be controlled and precise. The aim of this work is to obtain and characterize biocompatible micro and nanoparticulate systems based on a poly(D-lactic acid) matrix (PDLA) to study the controlled release of 1,4-naphthoquinone, which has reported anticancer activity. Scanning electron microscopy revealed spherical particles with an average size of 347 nm and 86% in the nanometer range. The encapsulation efficiency was 98.3%, as assessed by UV-visible spectroscopy. The hydrolytic degradation over 11 weeks showed controlled release of naphthoquinone at different pH conditions: 20.98% in alkaline, 19.69% in physiological, 18.83% in strongly acidic, and 16.70% in slightly acidic conditions. The enhanced release at alkaline pH suggests potential anticancer activity in colorectal cancer, benefiting treatment by releasing the drug to the affected area. Molecular docking studies on COX-2 confirmed these results, showing 1,4-naphthoquinone interacts with key amino acids (ALA202, THR206, HIS207) in the active site, modifying the prostaglandin chain which is crucial for the enzyme's function. The results show that this system has a high potential for use for pharmacological applications in colorectal cancer, as 1,4-naphthoquinone exhibits electronic properties.

Keywords: Controlled release. PDLA. 1,4-naphthoquinone. Micro and nanoparticles. Anticancer activity. Molecular docking.

¹Polymer Laboratory. Chemistry Center "Dr. Gabriel Chuchani." Venezuelan Institute of Scientific Research, Venezuela.

²Unit of Medicinal Chemistry. Faculty of Pharmacy. School "Dr. Jesus Maria Bianco." Central University of Venezuela. Caracas, Venezuela.

³School of Physics and Nanotechnology, Yachay Tech University. Ecuador.

⁴Center for Materials Engineering and Nanotechnology, Materials Laboratory. Venezuelan Institute of Scientific Research. Edo Miranda, Venezuela.

⁵Renato Archer Technology and Information Center, CTI. Campinas, SP, Brazil.

⁶B³IDA Group. Department of Chemistry. Simón Bolívar University. Edo Miranda, Venezuela.

Introduction

Controlled drug release is a very useful technique in pharmaceutical sciences, since it allows the drug to be released gradually and sustained in the body^{1,2}. Several mechanisms can accomplish this, including controlled diffusion, degradation of the encapsulating material, or response to specific stimuli (pH, temperature, enzymes)^{1,2}. Encapsulation is one of the primary strategies for controlling drug release, as an encapsulated drug has a number of benefits over other forms of administration and has been referred to as a modified drug release form³⁻⁶.

A key goal of medicinal chemistry is to improve the way in which active ingredients (such as biomolecules, drugs, etc.) are transported and released, thereby reducing side effects and improving therapeutic effects. As understanding of the pathophysiology of diseases and their cellular mechanisms is gained, drug delivery systems are customized in order to achieve optimal therapeutic effectiveness. The controlled drug release strategy allows the decrease of side effects, improve oral bioavailability, sustain the effect of drugs or genes in a selected tissue, increase the solubility of drugs for intravascular delivery and to improve the stability of therapeutic agents against enzymatic degradation by nucleases and proteases, especially in the case of drugs containing proteins, peptides, or nucleic acids^{3,7}.

From a pharmaceutical perspective, micro- and polymeric nanoparticles have the advantage of encapsulating lipophilic or hydrophilic substances at a high level. Moreover, they are used as vectors for the controlled release of proteins, peptides, vaccines, genes, and growth factors, among others, and in applications for a variety of therapies, including anticancer therapy⁸⁻¹⁰.

In the case of cancer therapy, the strategies adopted based on the use of micro- and nanoparticles have focused on two different mechanisms: A passive targeting strategy or vehiculization, and an active targeting strategy⁸. Passive targeting consists of the transport of micro-nanosystems through intracellular spaces into the tumor interstitium and their subsequent accumulation in these tissues. Active targeting refers to the active orientation of the micro-nanoparticles, and not just a simple accumulation in the tumor tissues, motivated by their marked specificity towards the target cells⁸. According to literature, the following biocompatible vehicles have been used to encapsulate drugs or biomolecules within particle matrixes: poly(L-lactic acid) (PLLA)⁹, poly(D-lactic acid) (PDLA)^{9,11,12}, polyethylene glycol (PEG)¹³, polyalkyl cyanoacrylate (PACA)¹⁴, poly-ε-caprolactone (PCL)¹⁵, poly(hydroxybutyrate-co-hydroxyvalerate) (PHBV)¹⁶, among others¹⁷. There are also polymethacrylates that react physicochemically to chan-

ges in pH, such as Eudragit^{®18}, which can be used to enhance oral drug bioavailability. Likewise, copolymers have been used, through the pegylation technique, being reported: PEG-PCL, PEG-PLA, among others^{19,20}. Nanocapsules have also been prepared using copolymers formed by varying the composition of their monomeric units of lactic acid/glycolic acid (PLGA)²¹⁻²³.

Poly(lactic acid)lactic acid, PLA, is an aliphatic polyester that have two stereoisomers PLLA and PDLA. The PDLA stereoisomer is amorphous and has been reported to decompose into non-toxic by-products through simple hydrolysis of the main ester chain in an aqueous environment, ultimately this degradation produces lactic acid which can be metabolized through the Krebs cycle into water and carbon dioxide^[24]. These characteristics make PDLA safe for use in tissue engineering applications and can be applied for the encapsulation and controlled drug released due to its ability to protect the drug from photodegradation and pH changes²⁴⁻²⁶.

Micro-nanoparticles have been produced using many methods based on different physical-chemical principles. Some of these methods are nanoprecipitation, emulsion diffusion, double emulsification, emulsion-coacervation, polymer coating, layering, etc.^{27,28}. The present research was conducted using the microemulsification technique^{29,30}, which is a modification of the original emulsion-diffusion process used by our research group. In most cases, polymeric particle sizes of nanometers³¹⁻³⁴, have been obtained, along with encapsulation values exceeding 90%^{11,35-37}.

In terms of drugs, this work highlights the use of the active compound naphthoquinone, which has been reported to have a wide range of derivatives with biological activities, especially against some cancer cell lines^{38,39}. Combined with their low toxicity, segments of these compounds have been proposed as potential cancer chemotherapeutics³⁸.

According to reports, chitosan membranes have been developed for the controlled release of 1,4-naphthoquinone to treat oncologic skin cancer wounds⁴⁰. In vitro studies have demonstrated its cytotoxic potential in colon cancer, human breast cancer, hepatocellular cancer, leukemia and human melanoma cells, producing induction of oxidative stress, apoptosis and cell membrane damage in these cell lines^{41,42}. Based on the results of these studies, this research is focused on evaluating the effects of PDLA micro- and nanoparticles released under controlled conditions³⁵.

As one of the most prevalent types of cancer in the world, colon-rectal cancer is one of the leading causes of morbidity and mortality. Approximately 10% of all cancer cases are caused by this disease,

and it is the second leading cause of cancer-related death. According to the World Health Organization (WHO), more than 1.9 million new cases of colorectal cancer and more than 930,000 deaths due to this disease were reported in 2020⁴³.

In colorectal cancer, many enzymes are overexpressed and represent potential targets of action. In this regard, it has been shown that the metabolism of arachidonic acid, a polyunsaturated fatty acid, either by the cyclooxygenase (COX) pathway or by the lipoxygenase (LOX) pathway, generates a series of proinflammatory substances called eicosanoids including prostaglandins, thromboxanes, leukotrienes⁴⁴. COX-2, in particular, plays a crucial role in inflammation and pain. Overexpression of cyclooxygenase-2 has been associated with several diseases, including colon cancer, where it can promote tumor growth and angiogenesis⁴⁵.

Studies have shown that colonic epithelial cells overexpressing the COX-2 gene resist apoptosis and exhibit altered adhesion and angiogenic properties. These findings suggest that COX-2 may be involved in colorectal cancer progression. Furthermore, COX-2 is elevated in 40% of colon adenomas and 90% of colon carcinomas, but not in normal colonic epithelium. Using human colon carcinoma cell lines, COX-2 has been shown to induce local immunosuppression by increasing prostaglandin E₂, a potent inhibitor of T-lymphocyte proliferation, which allows colon cancer cells to escape host immune defenses^{46,47}. Clinical studies have found that COX-2 selective nonsteroidal anti-inflammatory drugs (NSAIDs) have exhibited potent action in the treatment of colorectal cancer by inhibiting the cyclooxygenase enzyme, since they have the ability to reduce inflammation and pain without the side effects associated with nonselective NSAIDs, they are more effective as chemotherapeutic agents⁴⁸.

The use of *in silico* techniques in medicinal chemistry, such as molecular docking, to study the interaction of 1,4-naphthoquinone with enzymes overexpressed in colon cancer provides valuable information on the biochemical mechanisms that may influence its anticancer activity^[50]. These enzymes, involved in drug detoxification and metabolism processes, may modify the bioavailability and efficacy of the compound. By performing docking simulations, it is possible to identify the preferential binding sites and evaluate how structural modifications of naphthoquinone could optimize its interaction with these enzymes, potentially improving its therapeutic profile. By performing docking simulations, it is possible to identify the preferential binding sites and evaluate how structural modifications of naphthoquinone could optimize its interaction with these enzymes, potentially improving its therapeutic profile. Our goal was to evaluate the interaction

between 1,4-naphthoquinone and COX-2 enzyme by molecular docking analysis in order to correlate its previously reported anticancer activity^{[21], [22]} with its interaction with this enzyme. Additionally, our study focused on colon rectal cancer because the controlled release results obtained at alkaline pH, which corresponds to intestinal pH were higher⁴⁹.

Therefore, the objective of this study was to encapsulate 1,4-naphthoquinone in PDLA polymeric micro-nanoparticulate systems and release the drug selectively, as well as to correlate the biological activity of 1,4-naphthoquinone by molecular docking using the COX-2 enzyme.

Methodology

Reagents

1,4-naphthoquinone (C₁₀H₆O₂; molecular mass: 158.15 g/mol, 97% CAS No. 130-15-4 from Sigma-Aldrich) was used. For encapsulation, poly(D-Lactic acid) (PDLA), molecular mass ≈ 91102 g/mol, NatureWork USA, was used as a polymer. Polyvinyl Alcohol (PVA) (C₂H₄O)_n, molecular mass ≈ 9.5x10⁴ g/mol, CAS No. 9002-89-5, Himedia, was available. Deionized water, chloroform (CHCl₃; molecular mass: 119.38 g/mol, CAS No. 67-66-3, 99.5% purity from Sigma-Aldrich). All reagents were supplied without further purification. The materials were supplied by the Organic Chemistry Laboratory, B⁵IDA Group, Universidad Simón Bolívar.

Preparation of PDLA micro-nanoparticles by microemulsification

The methodology employed for the preparation of micro- and nanoparticles is presented below^{29,30}: A 100 mL solution of 0.025% m/v polyvinyl alcohol (PVA) in water was prepared. An additional 5.0 mL of a solution containing 1,4-naphthoquinone at 0.18% m/v in CHCl₃ and PDLA polymer solution at 1% m/v in CHCl₃ was added to this solution. The polymer solution with the 1,4-naphthoquinone was added using a micropipette. A finned reactor was used as a vessel and an ultradisperser was included. The reactor was immersed in ultrasound equipment for 120 min. After the process, the emulsion was left under continuous agitation for 24 hours to remove chloroform by evaporation. The resulting suspension was centrifuged. The precipitated particles were washed with deionized water to remove any PVA that may have remained on their surface. The wash water was retained to determine the percentage of encapsulation. Finally, the particles were lyophilized and prepared for characterization (See Figure 1).

Feasibility assay. Reduction of 3-(4,5-dimethylthiazol-2-yl)-5-(3-carboxymethoxyphenyl)-2-(4-sulfophenyl)-2H-tetrazolium salt (MTS) for PDLA micro-nanoparticles.

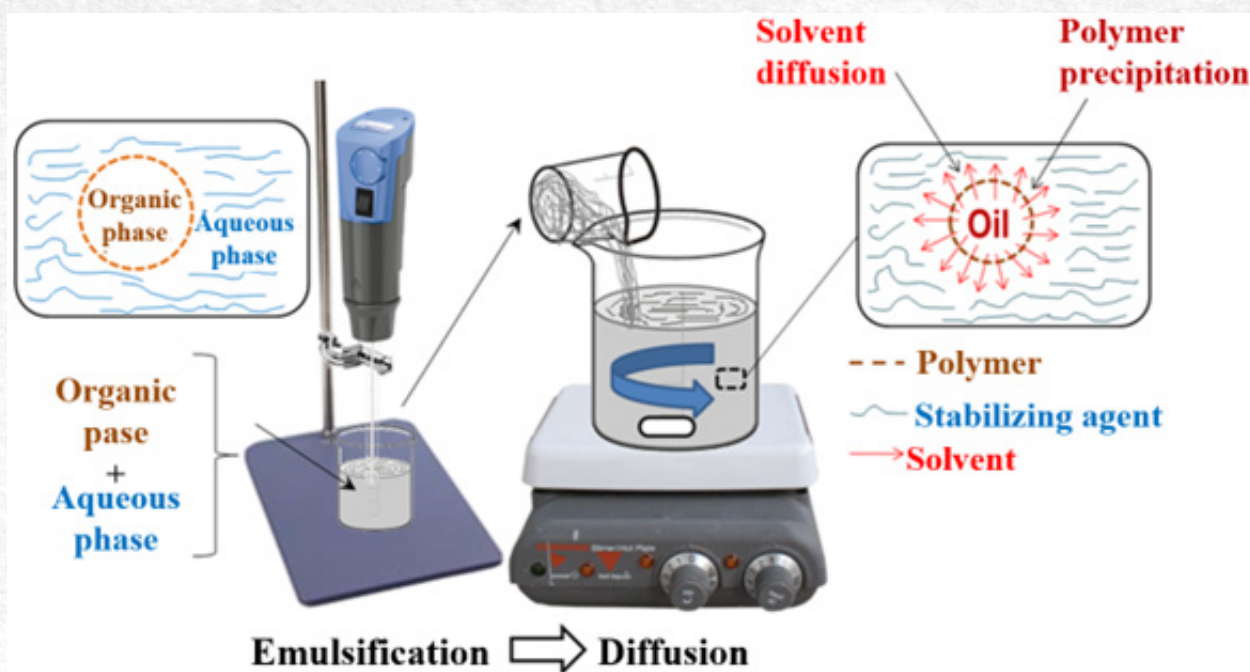


Figure 1 - Preparation of micro- and nanoparticles by emulsion-diffusion method.

PDLA polyester has been reported not to be cytotoxic [24], however, given the preparation method, it was necessary to evaluate the possible cytotoxicity of PDLA micro-nanoparticles without encapsulation. An *in vitro* cell survival study was previously performed, in MCF-7 breast cancer cells and NIH-3T3 murine fibroblasts, a colorimetric assay has been established for the metabolic reduction of MTS (reducing MTS to the tetrazolium salt [3-(4,5-dimethylthiazol-2-yl)-5-(3-carboxymethoxyphenyl)-2-(4-sulfophenyl)-2H-tetrazolium]) in formazan, and measuring the production of formazan at 550 nm⁵⁰.

To perform this, MCF-7 breast tumor cells and non-tumorigenic NIH-3T3 fibroblast cells were cultured at a density of 5x10³ cells per well in 96-well CELLSTAR® plates along with 100µL of DMEM medium supplemented with 15% SFB Gibco®, and left in incubation for 24 hours for adherence of the cells to the plate. Subsequently, the culture medium was removed and 90µL of the medium was added along with 10µL of the PDLA micro-nanoparticles at 1000 ppm concentration such that the concentration of the micro-nanoparticles in each well was 100 ppm. They were incubated at 37°C for 24, 48 and 72 hours, and at the end of this time 20µL of MTS CellTiter 96® Aqueous One Solution Cell Proliferation Assay G358A Promega® were added, waited 4 hours and the plates were read at 550 nm using the Autobio PHOMO® ELISA plate reader. As a positive control, cisplatin⁵¹ was used at different concentrations (0.5-100 µM). The assays were performed in triplicate.

Determination of encapsulation efficiency by UV-Visible Spectroscopy (UV-Vis)

The encapsulation efficiency of the compounds was determined indirectly from the quantification of the 1,4-naphthoquinone present in the washing water obtained after the encapsulation process in the micro and nanoparticles.

In this sense, an extraction of the derivatives contained in the washing water was carried out.

The organic solvent used in this experiment was chloroform, which promoted a liquid-liquid extraction and a saturated solution of NaCl. To determine the radiation absorption capacity of the compound obtained, the organic phase was dried using a rotary evaporator, and the compound obtained was diluted with DMSO to a volume of 2.0 mL. The calibration curves corresponding to the compounds were made, plotting the absorbance as a function of the concentration of each derivative. In order to determine encapsulation efficiency, 1,4-naphthoquinone absorption wavelength of 336nm according to equation (Eq.1)⁵²:

$$\% \text{ Encapsulation} = \frac{\text{Amount of encapsulated compound}}{\text{Initial amount of the compound in the system}} \times 100\% \text{ (Eq.1)}$$

UV-Vis controlled release assay by hydrolytic degradation at different pH conditions.

A hydrolytic degradation assay of polymeric micro-nanoparticles of 1,4-naphthoquinone was performed at different pH conditions, for this purpose:

a.- 10 mg of 1,4-naphthoquinone micro-nanoparticles in PDLA were placed in four centrifuge tubes at different conditions: acidic (1 ≤ pH ≤ 2), slightly acidic (pH ≈ 6), physiological (pH=7.4) and alkaline (pH=9). This model was made in virtue of being able to observe the different degradation conditions of these particles in pH that could occur in different

parts of the human body, for example, strongly acid gastric pH^[55], physiological pH in blood^[56], slightly acid pH in certain tumor conditions^[8] and slightly alkaline pH in the intestinal medium^[55].

b.- The assay was carried out for 12 weeks at 25 °C, during which the following extraction procedure was performed: the samples were centrifuged and a liquid-liquid extraction was performed in CHCl₃ and filtered with anhydrous MgSO₄.

c.- Each sample was brought to a volume of 2.00 mL for subsequent UV reading at the wavelength of maximum absorption ($\lambda=336\text{nm}$)^[52].

Characterization by Scanning Electron Microscopy

The PDLA micro-nanoparticles of 1,4-naphthoquinone, previously lyophilized, were observed using a JEOL JSM 6460 scanning electron microscope at 15 kV, previously, the samples were placed in a sample holder and coated with gold using a Balzers-SCD-030 Sputter-coater.

Molecular Docking Studies of 1,4-Naphthoquinone

For molecular docking studies the coordinates of Cyclooxygenase-2 (COX-2) were obtained from

the Protein Data Bank (PDBid: 5F1A). The PDB file of the enzyme was optimized by removing water molecules and co-crystallized ligands. The enzyme was energetically minimized in Swiss-PdbViewer (SPDBV) using GROMOS96 as the force field. Structural validation of the energetically minimized COX-2 was performed by Verify 3D using ERRAT, PROSA-WEB and ProCheck tools. Once the crystal structure of the receptor was validated, Molecular Docking studies were performed using AutoDock Vina and a ligand library consisting of 1,4-naphthoquinone (PubChem CID = 8530) and selective inhibitors (Parecoxib, PubChem CID = 119828; Sulindac, PubChem CID = 1548887; Rofecoxib, PubChem CID = 5090, Celecoxib; PubChem CID = 2662) and nonselective Cox-2 (Indomethacin, PubChem CID = 3715. All ligands were downloaded from PubChem in .sdf format and converted into .pdbqt formats to study molecular docking. Molecular docking studies were performed in quintuplicate. The results were prioritized according to the predicted binding free energy in kcal/mol. The molecular structure of the ligands used in the molecular docking studies is presented in Figure 2.

Results and Discussion

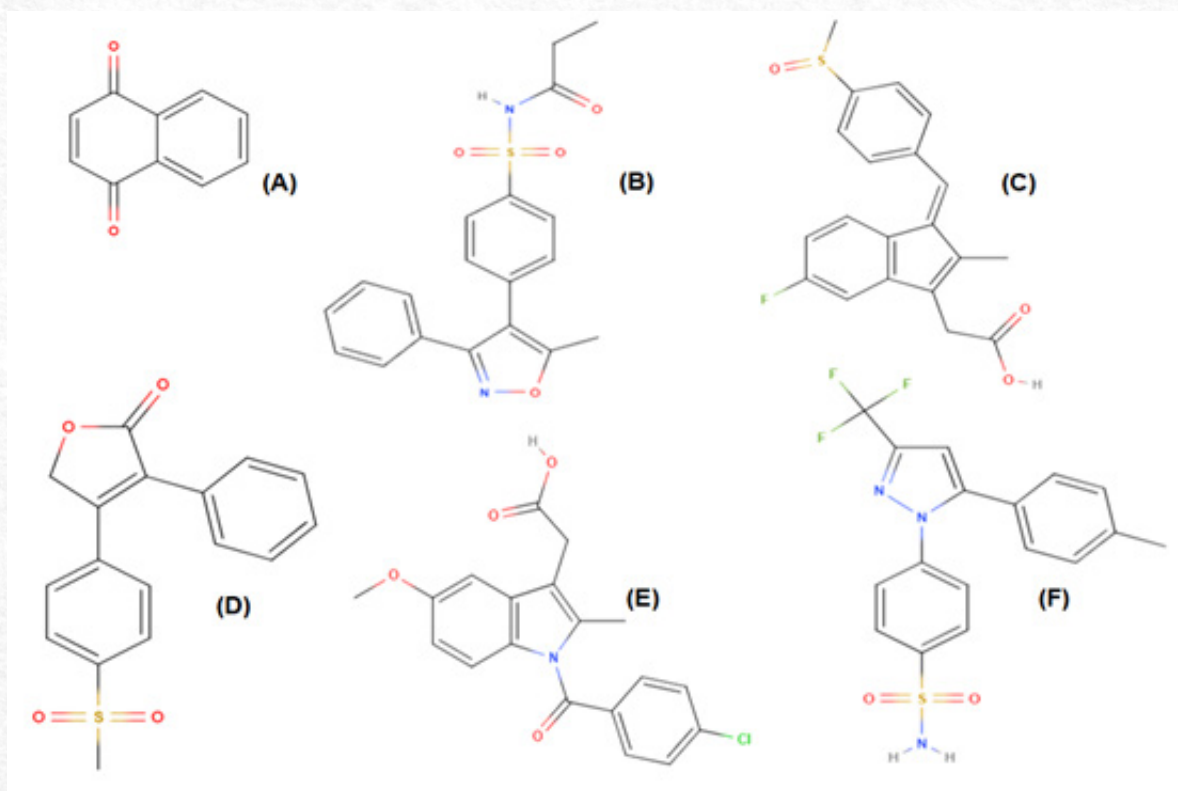


Figure 2 - Molecular structure of ligands and inhibitors used in molecular docking studies. 1,4-Naphthoquinone (A), Parecoxib (B), Sulindac (C), Rofecoxib (D), Indomethacin (E) and Celecoxib (F).

Encapsulation of 1,4-naphthoquinone in biocompatible polymeric micro-nanoparticles of PDLA by microemulsification

A previous analysis of the structure of 1,4-naphthoquinone and the polymer in which it was encapsulated, PDLA, indicates hydrogen bridge interactions can occur between the hydroxyl group

and the carbonyl group of PDLA and the carbonyl group of 1,4-naphthoquinone as shown in Figure 3. Moreover, 1,4-naphthoquinone is a flat aromatic molecule that can form a hydrophobic pocket during the formation of micro-nanoparticles.

Determination of encapsulation efficiency by UV-

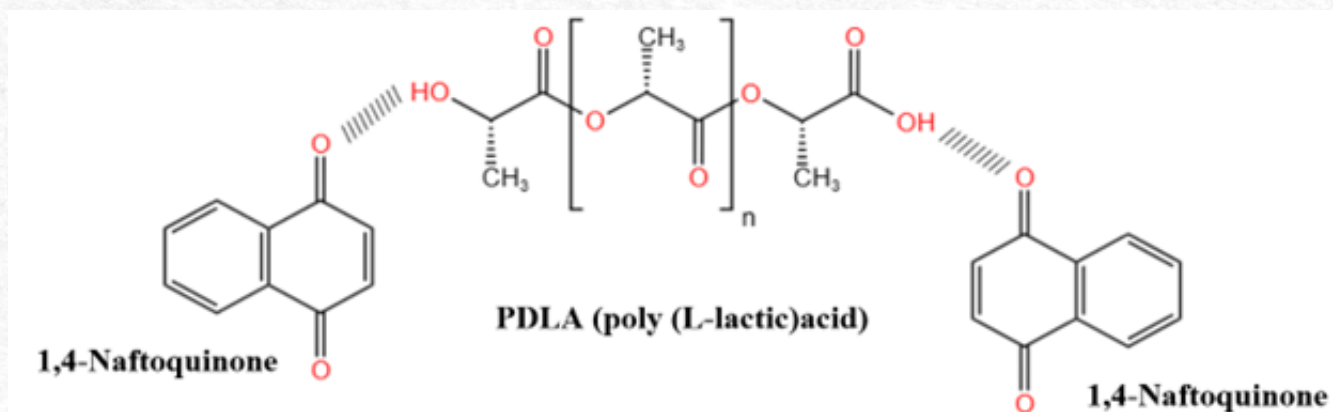


Figure 3 - Interactions between 1,4-naphthoquinone and PDLA polymer.

-Visible Spectroscopy

The value obtained for the encapsulation efficiency of 1,4-naphthoquinone in PDLA micro-nanoparticles is shown in Table 1. Based on the literature, the nanoprecipitation, emulsion-diffusion and layer-by-layer methods give the best results for

the encapsulation of micro-nanoparticles (80% or more)^{27,28}. A high percentage of encapsulation was obtained in this case, which is more than expected based on the literature.

Table 1 - Encapsulation efficiency of naphthoquinone in PDLA micro-nanoparticles.

Sample of 1,4-naphthoquinone/PDLA micro-nanoparticles	Added amount of compound	Encapsulated quantity	% Encapsulation
1,4-naphthoquinone	9 mg	8,8 mg	(98,3 ± 0,2)%

Characterization by Scanning Electron Microscopy

Scanning microscopy was used to determine the morphology of the micro and nanoparticles. Figure 4 shows the SEM images of the particles obtained without encapsulation, while Figure 5 shows the particles with the naphthoquinone encapsulated. As can be seen, the encapsulation process does not affect the morphology of the particles. Based on the microscopy results, the following average particle size distribution value was obtained for the 1,4-naphthoquinone micro-nanoparticles encapsulated (χ) in PDLA: $\chi = (347 \pm 10)$ nm. A symmetrical morphology of spherical particles and a particle size in the micro and nanometer range is observed presenting a higher percentage (86.12 %) in the nanometer scale, with adequate size dispersion and morphology which is favorable for the purposes of controlled release^{31-33,53-57}.

It is unclear what the particles look like inside, but based on the method used to obtain them, it is expected that they are similar to micronanospheres, that is, they are of the matrix type, in which drugs are dispersed within the particles, absorbed mostly on the surface of the spherical particles or encapsulated within the polymeric structures [11]. Based on our observations, the release of micro-nanoparticles prepared by emulsion-diffusion and emulsion-coacervation methods is faster⁹.

Cell viability assay: Metabolic reduction of

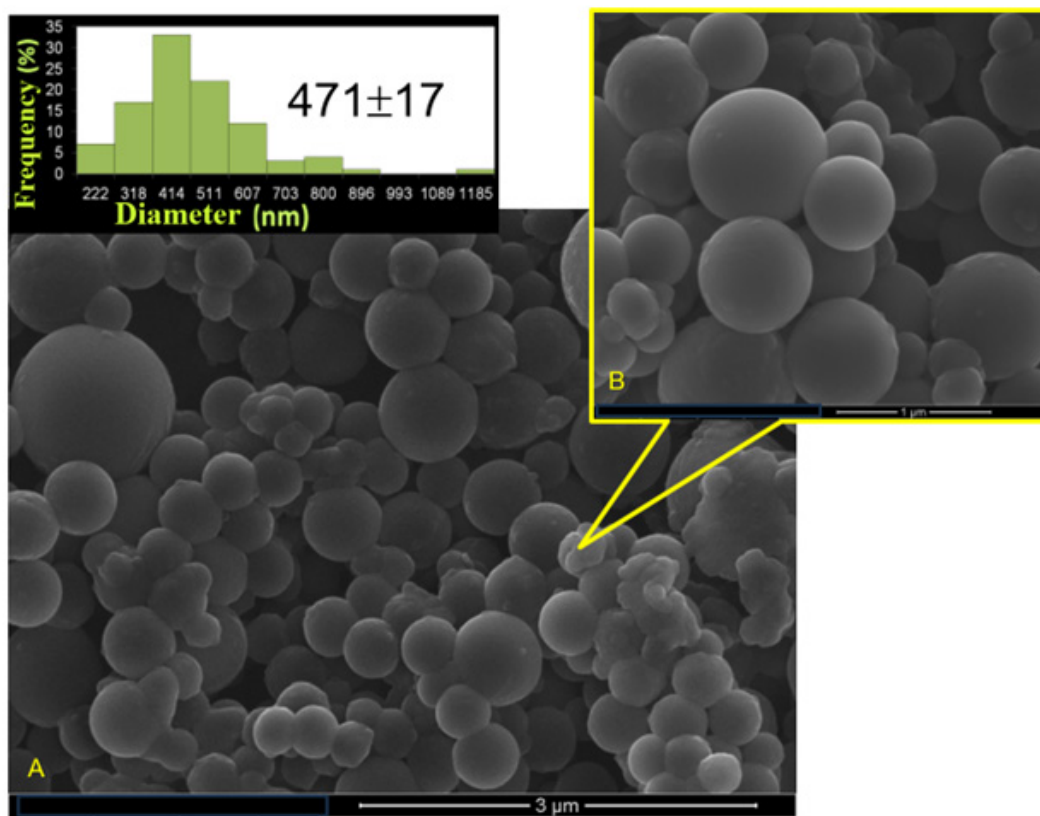


Figure 4 - SEM images: A) View of micro- and nanoparticles of PDLA. B) Details of the morphology.

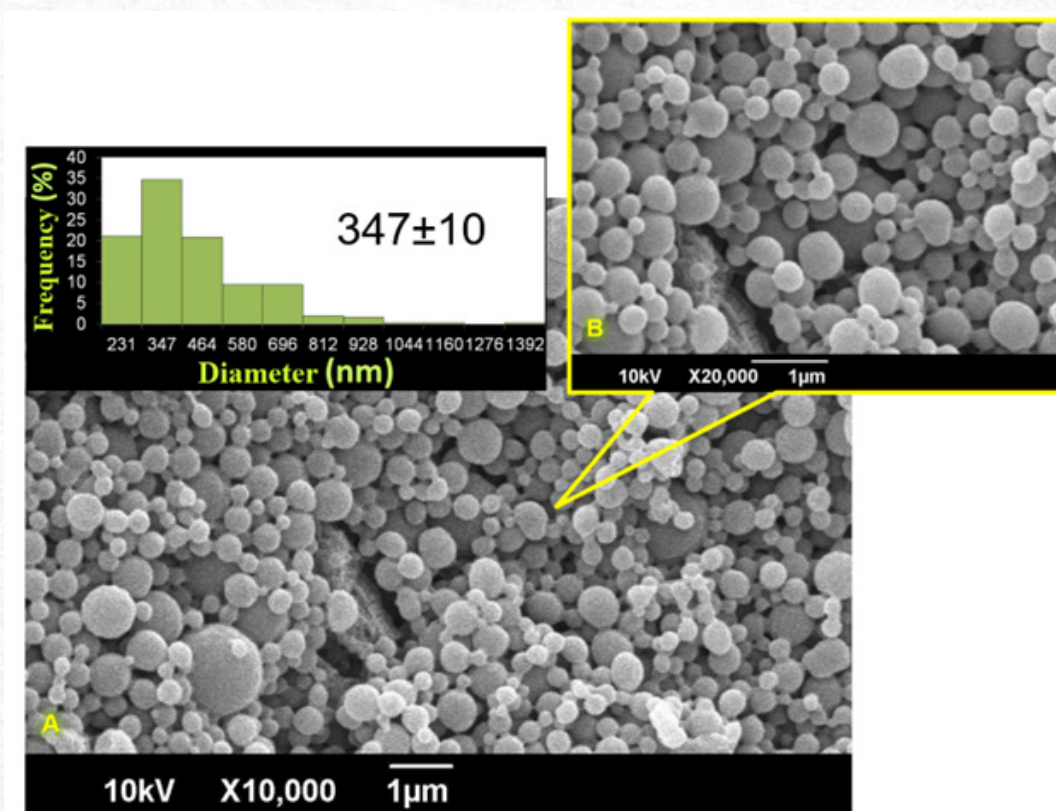


Figure 5 - SEM images: A) View of 1,4-naphthoquinone micro-nanoparticles encapsulated in PDLA. B) Details of the morphology.

3-(4,5-dimethylthiazol-2-yl)-5-(3-carboxymethoxyphenyl)-2-(4-sulfophenyl)-2H-tetrazolium salt (MTS)

The MTS cytotoxicity assay showed that at the maximum tested concentration of 100 ppm of the PLDA micro and nanoparticles did not show appreciable cell toxicity as they induced less than 5% cell death, in MCF-7 type breast cancer cells and in NIH-3T3 murine fibroblasts⁵⁰.

Release assay of 1,4-naphthoquinone in PDLA polymeric micro and nanoparticles by degradation test at different pH conditions

A degradation assay of the polymeric micro and nanoparticles was performed at different pH conditions and for 12 weeks at 25 °C: acidic ($1 \leq \text{pH} \leq 2$), slightly acidic ($\text{pH} \approx 6$), physiological ($\text{pH}=7.4$) and alkaline ($\text{pH}=9$) pH in order to be able to observe the different degradation conditions at pH of different parts of the human body, e.g. strongly acidic gastric pH, physiological pH in blood, slightly acidic pH in certain tumor conditions and slightly alkaline pH in the intestinal medium. The graph obtained from the 1,4-naphthoquinone release assay of PDLA polymeric micro and nanoparticles at different pH conditions is shown below in Figure 6.

As can be seen in the graph, at different pH conditions in the hydrolytic degradation of the PDLA micro and nanoparticles, a controlled release of 1,4-naphthoquinone was achieved for up to eleven weeks. It is observed that, at physiological pH, SBF medium, the peak is reached at the first week and remains constant until about the fifth week and

then rises; in alkaline medium the peak of release is reached at the second week and remains in constant ascent with respect to all other release profiles.

In slightly acidic medium, the release reaches a peak at week three, stabilizes until week five, and then increases further, finally in acidic medium the peak is reached at the second week and remains constant until about the fifth week and then rises.

The *in vitro* release process of an active substance from micro and nanoparticles depends on a variety of factors, such as the concentration and physicochemical characteristics of the active substance (in particular its solubility and oil/water partition coefficient); the nature, degradability, molecular mass and concentration of the polymer; the *in vitro* release test conditions (pH of the medium, temperature, contact time, among others) and the conditions of the preparation method⁹.

Micro and nanoparticles obtained by emulsion-diffusion methods are biphasic systems with an initial rapid release phase followed by a second slower release phase. Bursting is caused by desorption of active substances from micro and nanoparticle surfaces or by degradation of thin polymeric membranes. This behavior apparently exhibits zero-order kinetics⁹.

The second phase corresponds to the diffusion of the drug molecules from the inner compartment, the core of the reservoir, to the outer phase. This diffusion process seems to be determined by: the drug partition coefficient, the drug-polymer interactions and the surfactant concentration⁹.

This process does not appear to be limited by

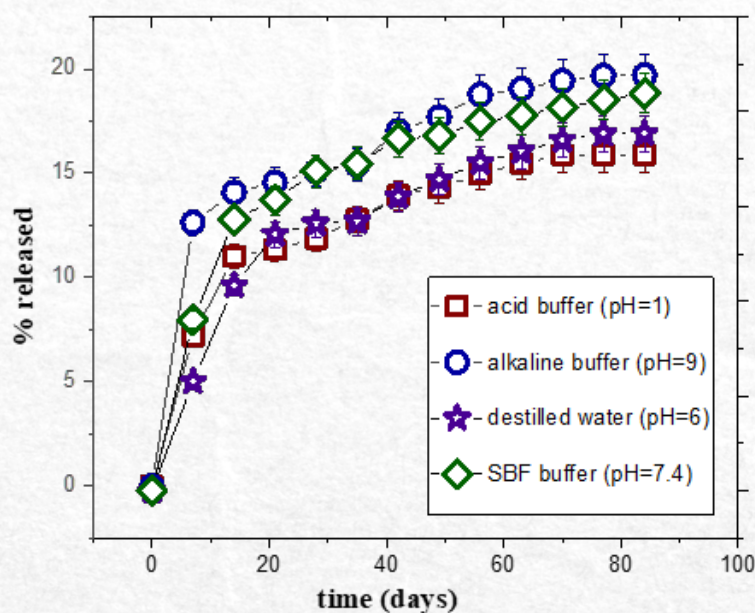


Figure 6 - % Released 1,4-naphthoquinone from PDLA micro-nanoparticles over time.

the rate of drug diffusion through the thin polymer barrier. The amount of polymer used can reduce the release rate significantly, and in such cases, erosion may facilitate drug release²⁸ by hydrolytic degradation, in this case.

In general, biodegradable polymers contain labile ester and anhydride bonds that are prone to hydrolysis⁶⁷, in the case of PDLA the hydrolysis-prone ester bond is observed. Polymers degrade hydrolytically when they come into contact with an aqueous medium, and depending on the pH of the medium, different degradation mechanisms occur. Upon penetration of water, the matrix swells, hydrogen bonds are broken, molecules are hydrated, and finally the unstable bonds are hydrolyzed. Hydrolysis may break functional groups on both the main chain and side chains^{68,69}.

Likewise, degradation of semicrystalline polymers occurs in two stages: i.) The first stage consists of the entry of water into the amorphous regions with random hydrolytic cleavage of labile bonds, such as ester bonds; ii.) Degradation of most amorphous regions marks the beginning of the second stage⁶⁷.

Having a good understanding of the degradation mechanism of polymeric materials offers the advantage of being able to predict its behavior and modify it accordingly. Therefore, several pH conditions were evaluated in the present assay. It is observed that at different pH conditions the hydrolytic degradation of the PDLA micro and nanoparticles exhibit kinetics that resembles zero order and that alkaline conditions accelerate the

degradation and therefore the release is favored, having the highest percentage of release being 20.98 %, followed by physiological medium at 19.69 %, strongly acid medium at 18.83% and slightly acid medium at 16.70%. There is evidence in the literature indicating that PLA degradation is favored at basic pH⁷⁰, which is in accordance with our results. Hydrolysis may be releasing lower molecular weight PLA chains and oligomers as degradation products. Consequently, hydrolytic degradation is favored from the inside out⁶⁹.

Acidic mediums have low degradation compared to basic mediums, possibly because amorphous zones and fragmented chains are predominantly attacked and do not diffuse into the medium until they become too small or diffuse in a negligible amount⁶⁹. From Figures 7 and 8, it can be seen that in basic media the mechanism occurs in fewer steps, which may influence the degradation rate, since the reaction takes place directly, largely because in the basic medium there is a strong base and nucleophile such as the hydroxyl ion (OH⁻) that is capable of directly attacking the acyl group, starting the hydrolysis process. Under acidic conditions, this situation does not occur, as activation of the acyl group under acid catalysis is required before the hydrolysis process can begin, giving rise to more stages, resulting in a wider variety of degradation by-products, however, the degradation process is slowed down even though primarily carboxylic acid groups and chain-terminal alcohols are obtained at the end⁷¹⁻⁷⁴.

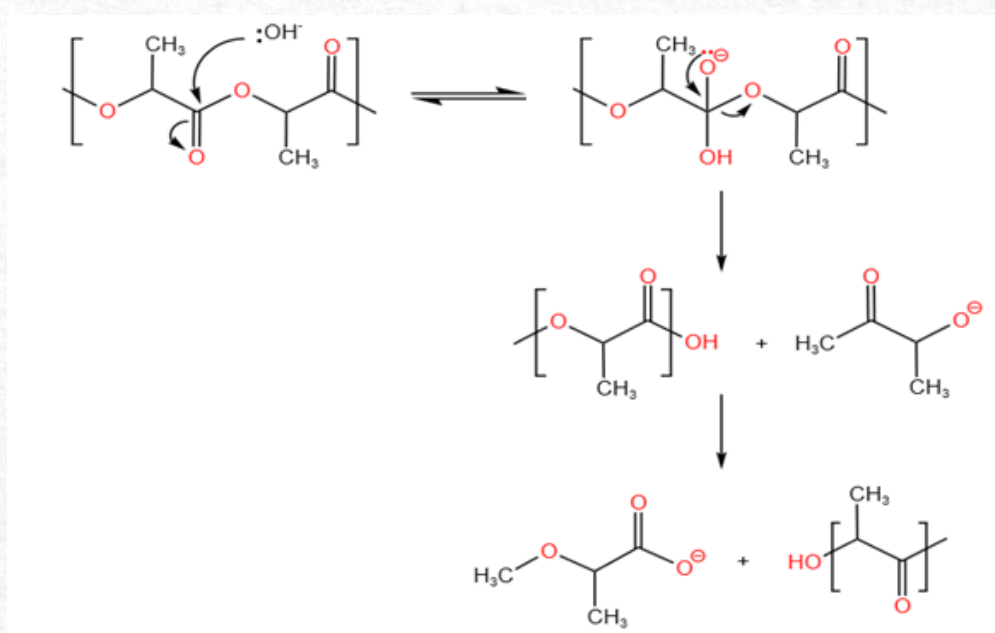


Figure 7 - Proposed mechanism of PDLA degradation by basic hydrolysis. Modified from references⁷¹⁻⁷⁴.

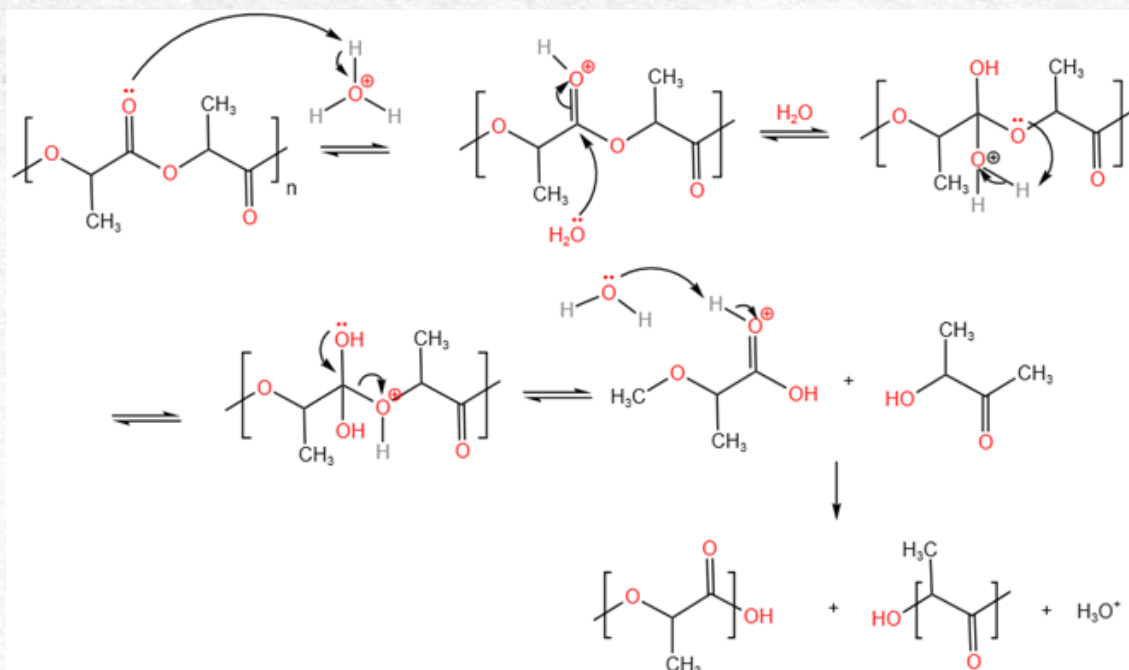


Figure 8 - Proposed mechanism of PDLA degradation by acid hydrolysis. Modified from references⁷¹⁻⁷⁴.

Hence, this study demonstrated that the hydrolytic degradation of polymeric micro and nanonanoparticles during 12 weeks at 25 °C under different pH conditions, demonstrated controlled release of naphthoquinone at different pH conditions over a period of 11 weeks, which is crucial for potential applications in colorectal cancer treatment. Different pH levels, including acidic, slightly acidic, physiological, and alkaline conditions, mimic the gastrointestinal tract and tumour microenvironments. Based on their release patterns, the PDLA micro and nanoparticles have demonstrated a high degree of efficiency in delivering 1,4-naphthoquinone, especially in the alkaline conditions found in the small intestine, where the release rate was highest (20.98%). This is noteworthy, since the small intestine is an important site of drug absorption, and the controlled release of 1,4-naphthoquinone in this region might enhance its therapeutic efficacy against colorectal cancer. The release profiles at different pH levels may also be relevant to the tumour microenvironment, where pH levels can vary significantly. By using PDLA micro and nanoparticles to release 1,4-naphthoquinone in a pH-dependent manner, the drug's anticancer properties may be enhanced and exploited to target specific regions of the tumour. PDLA micro and nanoparticles are a promising drug delivery system for the treatment of colorectal cancer, based on these findings.

Molecular Docking Studies

A docking study was conducted on

1,4-naphthoquinone to assess its potential therapeutic effects on colorectal cancer. At alkaline pH, 1,4-naphthoquinone was released more efficiently, suggesting better absorption in the small intestine. The incidence of colorectal cancer is the third highest in the world and is more prevalent in older individuals and people of all ages⁷⁵.

A potential therapeutic target has been identified as Cyclooxygenase-2 (COX-2) due to its role in promoting tumor growth, angiogenesis (the formation of new blood vessels that feed tumors) and inhibiting apoptosis (programmed cell death)⁷⁶. According to previous clinical studies, non-steroidal anti-inflammatory drugs (NSAIDs) are effective in treating colorectal cancer by inhibiting the enzyme cyclooxygenase. Further research concluded that cyclooxygenase-2 (COX-2) gene inhibitors are most effective for chemotherapy treatment⁷⁷. By inhibiting COX-2, selective cyclooxygenase-2 (COX-2) inhibitors, better known as coxibs, can reduce inflammation, pain, cancer cell proliferation, and new blood vessel formation, all of which can slow tumor growth without affecting the gastric protective effect provided by COX-1^{76,78}. These compounds work by blocking the action of COX-2, an enzyme that is overexpressed in inflamed tissues and in certain types of cancer, such as colorectal cancer^{76,78}. The most effective when used in conjunction with COX-2 inhibitors such as Parecoxib, Sulindac, Rofecoxib, and Celecoxib^{77,79}.

Molecular docking was performed by first downloading the COX-2 enzyme (PDBid: 5F1A) from the Protein Data Bank (<https://www.rcsb.org/>

structure/5F1A) and energetically minimizing it in order to: a) relax the structural stresses presented by inducing forced crystallization experimentally of the enzyme, providing a more realistic and stable conformation of the receptor⁸⁰, b) an energetically minimized receptor structure allows better prediction of the ligand-receptor interaction. This is essential to obtain accurate results in terms of binding affinity and ligand orientation⁸¹, and c) minimization facilitates ligand accommodation in receptor active sites, which improves interaction^{80,81}.

As soon as the enzyme was minimized, it was validated using three different tools (ERRAT⁵⁶, Prosa-Web⁵⁷, and ProCheck⁵⁸) to analyze the quality of the receptor structure. Resulting in an Overall Quality Factor of 97.026 in ERRAT, a Z-Score of -8.62 in Prosa-Web⁵⁷, and a total of 89.5% of residues in favorable zones according to the Ramachandran Plot reported in ProCheck⁵⁸ (for additional information please refer to the supplementary material).

Co-crystallized ligand was used as a positive control to verify that the selected box contained the essential amino acids of the active site. Certain amino acids, such as Ala202, Thr206, His 207, Val291, Pro441, Ala443, Val444, Lys446, Ser448 and Ala450, play crucial roles in the binding process of COX-2^{77,82}. A library of six ligands was run, including 1,4-naphthoquinone, selective COX-2 inhibitors (Parecoxib, Sulindac, Rofecoxib, Celecoxib) and non-selective COX-2 inhibitors (Indomethacin). The results of the quintuplicate molecular docking studies are presented in Table 2.

Based on the results presented in Table 2, it appears that, Parecoxib (-9.70 Kcal/mol) is the selective COX-2 inhibitor that presents the lowest binding energy and consequently; higher interaction with COX-2. Despite its weaker affinity for COX-2 (-7.32 Kcal/mol) than other COX-2 inhibitors, 1,4-naphthoquinone may be useful when moderate inhibition is desired.

By inhibiting COX-2 and regulating inflammatory prostaglandin production, 1,4-naphthoquinone could reduce inflammation and relieve pain, as it interacts with essential amino acids in the COX-2 active site such as ALA-202 (via π -alkyl interactions), THR-206 (via hydrogen bridge-type interactions), HIS-207 (via π donor-hydrogen bond) and HIS-386 (via π - π stacked interactions). Figure 9A shows the pocket of 1,4-naphthoquinone in COX-2 constructed using ICM Mol-Soft; Figure 9B presents the 2D interaction diagram generated in Discovery Studio for the best pose 1,4-naphthoquinone; Figure 9C, the selective COX-2 inhibitor parecoxib (gray color) and 1,4-naphthoquinone (yellow color) are shown overlaid to indicate that both ligands reside in the same active site. Parecoxib, however, being a more voluminous ligand, extends more in the active site, resulting in a greater complementarity with the cavity, and hence having a higher affinity and greater inhibitory activity.

Despite its rather simple molecular structure consisting of two rings (one aromatic and one aliphatic), 1,4-naphthoquinone has been shown to moderately inhibit COX-2, acting as a chemotherapeutic in colorectal cancer.

Furthermore, 1,4-naphthoquinone can serve as a starting point for chemical synthesis of other ligands and is in principle a potential lead compound as it does not violate the Lipinski rules calculated by SwissADME^{83w} (<http://www.swissadme.ch/index.php>) (see supplementary material). Based on *in silico* studies, three new ligands were proposed, introducing hydroxyl and methoxide groups around the aromatic ring to improve hydrogen bonding and lipophilicity. The small changes resulted in a significant increase in inhibitory capacity for COX-2, which increased affinity energy by 0.48 Kcal/mol (5-methoxy-1,4-naphthoquinone), making it more effective as a chemotherapeutic agent (Figure 10).

Table 2 - Ligand-receptor interaction energy (COX-2) obtained through molecular docking studies.

	Run 1	Run 2	Run 3	Run 4	Run 5	Average	Desvest
Ligand	Affinity Energy (Kcal/mol)	Affinity Energy (Kcal/mol)	Affinity Energy (Kcal/mol)	Affinity Energy (Kcal/mol)	Affinity Energy (Kcal/mol)	(Kcal/mol)	(Kcal/mol)
Parecoxib	-9.70	-9.70	-9.60	-9.80	-9.70	-9.70	0.07
Celecoxib	-9.40	-9.50	-9.40	-9.40	-9.50	-9.44	0.05
Sulindac	-9.10	-9.00	-9.00	-9.00	-9.00	-9.02	0.04
Indomethacin	-8.80	-8.81	-8.80	-8.79	-8.81	-8.80	0.01
Rofecoxib	-8.70	-8.70	-8.60	-8.70	-8.60	-8.66	0.05
1,4-Naphthoquinone	-7.30	-7.30	-7.40	-7.30	-7.30	-7.32	0.04

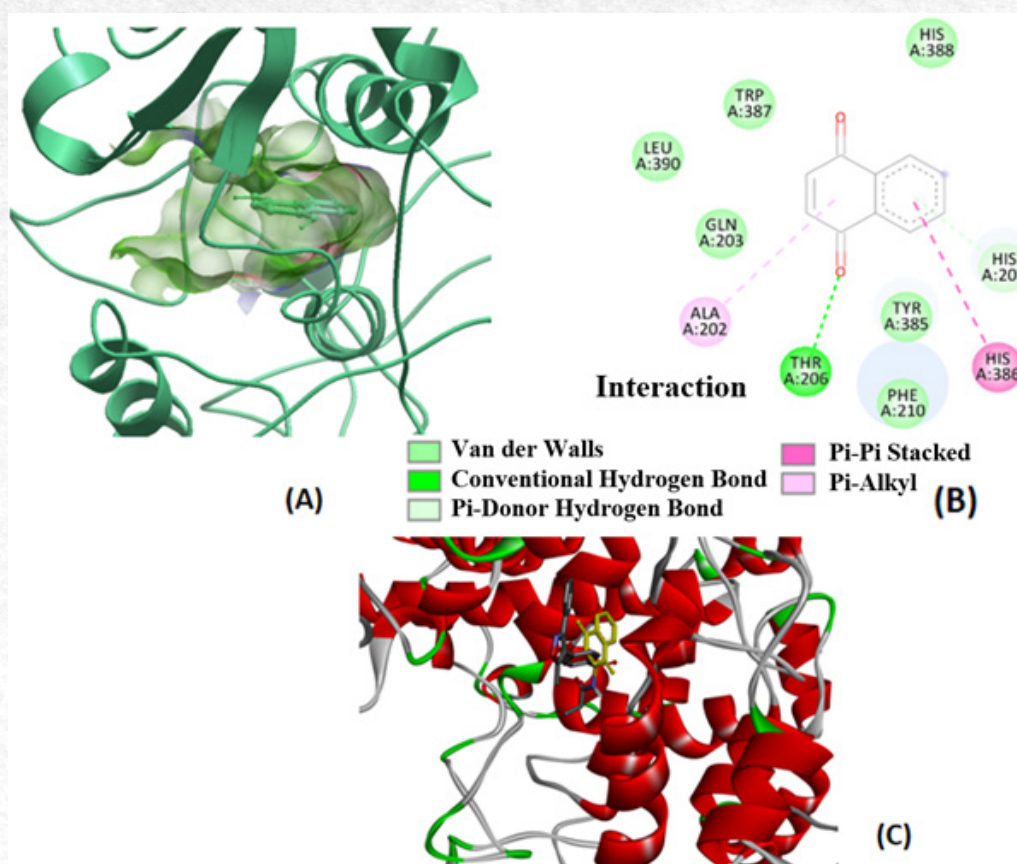


Figure 9 - 1,4-Naphthoquinone-COX-2 interaction pocket (A). 2D ligand-receptor interaction diagram (B). Overlap of Parecoxib (grey) and 1,4-naphthoquinone (yellow) in the active site (C).

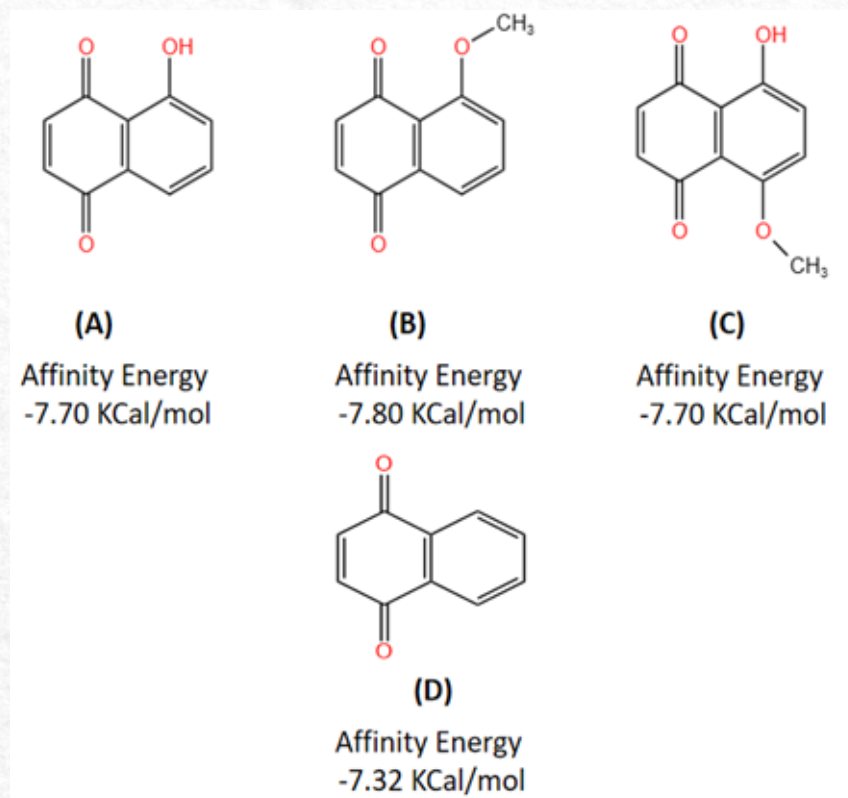


Figure 10 - Increase in affinity energy of modified 1,4-Naphthoquinone ligands. 5-hydroxy-1,4-naphthoquinone (A), 5-methoxy-1,4-naphthoquinone (B), 5-hydroxy-8-methoxy 1,4-naphthoquinone (C), 1,4-naphthoquinone (D).

Conclusions

A remarkable 98.3% encapsulation rate was achieved for 1,4-naphthoquinone in PDLA micro and nanoparticles. MTS assays conducted on MCF-7 breast cancer cells and NIH-3T3 murine fibroblasts demonstrated that the PDLA polymeric micro and nanoparticles were not toxic at concentrations up to 100 ppm. A controlled release assay revealed that alkaline conditions accelerated the degradation of micro and nanoparticles, resulting in a higher release percentage. Under the tested conditions, the system maintained a controlled release for eleven weeks. PDLA based drug delivery systems have significant potential for pharmacological applications, particularly for treating colorectal cancer. Molecular docking studies have demonstrated that 1,4-naphthoquinone can inhibit COX-2 by altering the mechanism of prostaglandin production which is valuable for developing novel anti-inflammatory drugs, exhibiting potential chemotherapeutic activity. Alone or combined with other inhibitors, 1,4-naphthoquinone could be a valuable chemotherapeutic agent, inhibiting COX-2, a key enzyme in colorectal cancer. PDLA micro and nanoparticles encapsulated with 1,4-naphthoquinone offer a promising approach for achieving controlled drug release in the treatment of colorectal cancer. By delivering drugs in a sustained and targeted manner, the system may be able to enhance therapeutic efficacy and reduce side effects. Future research should focus on *in vivo* studies to evaluate the efficacy and safety of PDLA based drug delivery systems. Furthermore, combining therapies and optimizing micro and nanoparticle encapsulation and design could improve drug delivery efficiency and effectiveness. This study underscores the potential of PDLA based drug delivery systems to revolutionize cancer treatment, particularly in colorectal cancer. Developing these systems will lead to improved therapeutic outcomes and more effective and personalized cancer therapies.

Acknowledgments

This article is dedicated to honoring the memory of Dr. Jorge Vicente Lopes da Silva, he passed away before the submission of this study, and who was an important pillar for the B⁵IDA research group at Universidad Simón Bolívar (USB) and for his invaluable collaboration throughout; including his contributions to the conceptualization and visualization of this research.

The authors would like to thank: Lic. Gleen Rodríguez at the Surface Lab of Lab E of USB for the preparation and observation of samples by SEM. To Dr. Juan Rodríguez of the

Cell Biology Lab. at USB for performing the cell viability assays. Lic. Damaris Soto from Center for Materials Engineering and Nanotechnology of the Venezuelan Institute of Scientific Research (IVIC) for supporting the UV-visible assays. CNPq-Brazil PCI program (process #300933/2024-0) for the financial support. And finally, express gratitude to the Fondo Nacional de Ciencia Tecnología e Innovación (FONACIT) for the funding received from projects # 2022OPGP125 and 2023PGP99.

References

- [1]. Zárate-Hernández, E., Hernández-Esquivel, R. A. & Pérez-Urizar, J. T. Microcapsules and microspheres: A vision to integral characterization and applications for biotechnological drugs delivery. *CienciaUAT* 15, (2021).
- [2]. Puccetti, M., Pariano, M., Schoubben, A., Giovagnoli, S. & Ricci, M. Biologics, theranostics, and personalized medicine in drug delivery systems. *Pharmacol. Res.* 201, (2024).
- [3]. Villafuerte-Robles, L. *Nanotecnología Farmacéutica. Razón y Palabra* 68, 1–20 (2009).
- [4]. Chapters, G. et al. Revisions to USP 30-NF 25 , First Supplement. (2011). USP XXXVIII NF XXXII.
- [5]. Liaqat, S. et al. Doxorubicin encapsulated blend of sitagliptin-lignin polymeric drug delivery system for effective combination therapy against cancer. *Int. J. Biol. Macromol.* 269, 132146 (2024).
- [6]. Kita, K. & Dittrich, C. Drug delivery vehicles with improved encapsulation efficiency: Taking advantage of specific drug-carrier interactions. *Expert Opin. Drug Deliv.* 8, 329–342 (2011).
- [7]. Lollo, G. Nanocápsulas de poliaminoácidos para la liberación selectiva de fármacos antitumorales. 346 (2012).
- [8]. Thauvin, C., Schwarz, B., Delie, F. & Allémann, E. Functionalized PLA polymers to control loading and/or release properties of drug-loaded nanoparticles. *Int. J. Pharm.* 548, 771–777 (2018).
- [9]. Kanaoujiya, R., Kumar Sahu, D., Behera, K., Kumar Singh, S. & Srivastava, S. Biomedical application of polymer based nanomaterials: Vaccines & drugs. *Mater. Today Proc.* (2023). doi:10.1016/j.matpr.2023.03.824
- [10]. González R, K. N., González, G., Rodríguez, J., Marques, Kruzakaya Vázquez, A. S. & Sabino, M. A. Encapsulación de derivados de sulfanil – sulfonil chalconas en sistemas micro/nanoparticulados poliméricos de PDLA con aplicación de liberación controlada. *Mater. Simulación Procesos Ind. y Nanotecnología JIFI-EAI*, (2018).
- [11]. González, K. N., González, G. & Sabino, M. A. Preparation of micro and nanoparticulated systems

- based in degradable polyesters for encapsulation of hirudin and delivery. *Acta Microsc.* 32, 29–38 (2023).
- [12]. Lee, J. Y., Bae, K. H., Kim, J. S., Nam, Y. S. & Park, T. G. Intracellular delivery of paclitaxel using oil-free, shell cross-linked HSA - Multi-armed PEG nanocapsules. *Biomaterials* 32, 8635–8644 (2011).
- [13]. Alhareth, K., Vauthier, C., Gueutin, C., Ponchel, G. & Moussa, F. HPLC quantification of doxorubicin in plasma and tissues of rats treated with doxorubicin loaded poly(alkylcyanoacrylate) nanoparticles. *J. Chromatogr. B Anal. Technol. Biomed. Life Sci.* 887–888, 128–132 (2012).
- [14]. Oliveira, A. I., Pinho, C., Fonte, P., Sarmiento, B. & Dias, A. C. P. Development, characterization, antioxidant and hepatoprotective properties of poly(ϵ -caprolactone) nanoparticles loaded with a neuroprotective fraction of *Hypericum perforatum*. *Int. J. Biol. Macromol.* 110, 185–196 (2018).
- [15]. Puppi, D., Braccini, S., Ranaudo, A. & Chiellini, F. Poly(3-hydroxybutyrate-co-3-hydroxyhexanoate) scaffolds with tunable macro- and microstructural features by additive manufacturing. *J. Biotechnol.* 308, 96–107 (2020).
- [16]. Karlsson, J., Vaughan, H. J. & Green, J. J. Biodegradable Polymeric Nanoparticles for Therapeutic Cancer Treatments. *Annu. Rev. Chem. Biomol. Eng.* 9, 105–127 (2018).
- [17]. Tian, S. et al. Controlled drug delivery for glaucoma therapy using montmorillonite/Eudragit microspheres as an ion-exchange carrier. *Int. J. Nanomedicine* 13, 415–428 (2018).
- [18]. Nosrati, H., Adinehvand, R., Manjili, H. K., Rostamizadeh, K. & Danafar, H. Synthesis, characterization, and kinetic release study of methotrexate loaded mPEG–PCL polymersomes for inhibition of MCF-7 breast cancer cell line. *Pharm. Dev. Technol.* 24, 89–98 (2019).
- [19]. Pan, L., Zhou, J., Ju, F. & Zhu, H. Intranasal delivery of α -asarone to the brain with lactoferrin-modified mPEG-PLA nanoparticles prepared by premix membrane emulsification. *Drug Deliv. Transl. Res.* 8, 83–96 (2018).
- [20]. Saez, V., Hernández, J. R. & Peniche, C. Las microesferas como sistemas de liberación controlada de péptidos y proteínas. *Biotechnol. Apl.* 24, 98–107 (2007).
- [21]. Moraes, C. M., Paula, E. De, Rosa, A. H. & Fraceto, L. F. Physicochemical stability of poly(lactide-co-glycolide) nanocapsules containing the local anesthetic bupivacaine. *J. Braz. Chem. Soc.* 21, 995–1000 (2010).
- [22]. Budama-Kilinc, Y. et al. Novel NAC-loaded poly(lactide-co-glycolide acid) nanoparticles for cataract treatment: Preparation, characterization, evaluation of structure, cytotoxicity, and molecular docking studies. *PeerJ* 2018, (2018).
- [23]. Hubbell, J. Biomaterials in tissue engineering. *Biotechnology* 565–76 (1995).
- [24]. Wang, S., Tan, M., Zhong, Z., Chen, M. & Wang, Y. Nanotechnologies for Curcumin: An Ancient Puzzler Meets Modern Solutions. *J. Nanomater.* 2011, 8 (2011).
- [25]. Yasukawa, T., Tabata, Y., Kimura, H. & Ogura, Y. Recent Advances in Intraocular Drug Delivery Systems. *Recent Pat. Drug Deliv. Formul.* 5, 1–10 (2011).
- [26]. Yu, B. et al. Morphology and internal structure control over PLA microspheres by compounding PLLA and PDLA and effects on drug release behavior. *Colloids Surfaces B Biointerfaces* 172, 105–112 (2018).
- [27]. Mora-Huertas, C. E., Fessi, H. & Elaissari, A. Polymer-based nanocapsules for drug delivery. *Int. J. Pharm.* 385, 113–142 (2010).
- [28]. Crucho, C. I. C. & Barros, M. T. Polymeric nanoparticles: A study on the preparation variables and characterization methods. *Mater. Sci. Eng. C* 80, 771–784 (2017).
- [29]. Vanderhoff, J., Mohamed, S. & Ugelstad, J. Polymer Emulsification Process.
- [30]. Vanderhoof, J., Vitkuske, F. & Bradford, E. Uniform Particle Size Latexes *. *J. Polym. Sci.* 20, 225–234 (1956).
- [31]. Lockman, P. R., Mumper, R. J., Khan, M. A. & Allen, D. D. Nanoparticle technology for drug delivery across the blood-brain barrier. *Drug Dev. Ind. Pharm.* 28, 1–13 (2002).
- [32]. Brigger, I., Dubernet, C. & Couvreur, P. Nanoparticles in cancer therapy and diagnosis. *Adv Drug Deliv Rev* 54, 631–651 (2002).
- [33]. Palma, E. et al. Antileishmanial activity of amphotericin B-loaded-PLGA nanoparticles: An overview. *Materials (Basel)*. 11, (2018).
- [34]. González, K. et al. In vitro anti-trypanosomal activity of 3-(aryl)-6-piperazinyl,2,4-triazolo[3,4- a] phthalazines-loaded ultrathin polymeric particles: effect of polymer type and particle size. *RSC Pharm.* (2024). doi:10.1039/d3pm00002h
- [35]. Karina Noreica, G. R. Síntesis y desarrollo de sistemas micro y nanoestructurados para la liberación controlada de fármacos. (Universidad Central de Venezuela, 2022).
- [36]. Marcano, Y. C. & Sabino, M. A. G. Chemical modification of alginate with L-cysteine to extend its use in drug delivery systems. *Cellul. Chem. Technol.* 52, 559–567 (2018).
- [37]. López, L., Leyva, E., La, G. de & Cruz, R. Las naftoquinonas : más que pigmentos naturales. *Rev. Mex. ciencias Farm.* 42, 1–17 (2011).
- [38]. Wang, S. H. et al. Synthesis and biological evaluation of lipophilic 1,4-naphthoquinone derivatives against human cancer cell lines. *Molecules* 20, 11994–12015 (2015).

- [39].Tomaz, A. F. et al. Ionically crosslinked chitosan membranes used as drug carriers for cancer therapy application. *Materials (Basel)*. 11, 1–18 (2018).
- [40].Kumar, D., Gihar, S., Shrivash, M. K., Kumar, P. & Kundu, P. P. A review on the synthesis of graft copolymers of chitosan and their potential applications. *Int. J. Biol. Macromol.* 163, 2097–2112 (2020).
- [41].Klaus, V. et al. 1,4-Naphthoquinones as inducers of oxidative damage and stress signaling in HaCaT human keratinocytes. *Arch. Biochem. Biophys.* 496, 93–100 (2010).
- [42].OMS. Cáncer colorrectal. (2023). Available at: <https://www.who.int/es/news-room/fact-sheets/detail/colorectal-cancer>. [accessed 4 June 2024]
- [43].Soumaoro, L. T. et al. Expression of 5-lipoxygenase in human colorectal cancer. *World J. Gastroenterol.* 12, 6355–6360 (2006).
- [44].Jin, K., Qian, C., Lin, J. & Liu, B. Cyclooxygenase-2-Prostaglandin E2 pathway: A key player in tumor-associated immune cells. *Front. Oncol.* 13, 1–10 (2023).
- [45].Gómez Estrada, H. A., González Ruiz, K. N. & Medina, J. D. Actividad antiinflamatoria de productos naturales. *Bol. Latinoam. y del Caribe Plantas Med. y Aromat.* 10, 182–217 (2011).
- [46].Gonzalez-Angulo, A. M., Fuloria, J. & Prakash, O. Cyclooxygenase 2 inhibitors and colon cancer. *Ochsner J.* 4, 176–179 (2002).
- [47].Yadav, M. et al. Structure-Based Virtual Screening, Molecular Docking, Molecular Dynamics Simulation and Pharmacokinetic modelling of Cyclooxygenase-2 (COX-2) inhibitor for the clinical treatment of Colorectal Cancer. *Mol. Simul.* 1081–1101 (2022). doi:<https://doi.org/10.1080/08927022.2022.2068799>
- [48].Abdelaziz, A. A. S. et al. Molecular docking and Anticancer Activity of Some Synthesized 1,4- naphthoquinone Derivatives against Human Cancer Cell Line. *J. Mol. Struct.* 1275, 134702 (2023).
- [49].Mosmann, T. Rapid colorimetric assay for cellular growth and survival: Application to proliferation and cytotoxicity assays. *J. Immunol. Methods* 65, 55–63 (1983).
- [50].Quispe, M. A. et al. Actividad citotóxica de *Physalis peruviana* (aguaymanto) en cultivos celulares de adenocarcinoma colorrectal, próstata y leucemia mieloide crónica. *Rev. Gastroenterol. del Perú.* 29, 239–46 (2009).
- [51].García F, P. T. Propiedades opticas de Naftoquinonas N-Fenil sustituidas. (Universidad Nacional Autónoma de México, 2007).
- [52].Garcia, M. Disturbios del estado ácido-básico en el paciente crítico. *Acta Med Per* 28, 46–55 (2011).
- [53].Hanna. ¿Cuáles son los niveles de pH del cuerpo humano? (2022). Available at: <https://www.hannainst.es/blog/1533/cuales-son-los-niveles-de-ph-del-cuerpo-human>.
- [54].Guex, N., Peitsch, M. C. & Schwede, T. Automated comparative protein structure modeling with SWISS-MODEL and Swiss-PdbViewer: A historical perspective. *Electrophoresis* 30, 162–173 (2009).
- [55].Colovos, C. & Yeates, T. O. Verification of protein structures: Patterns of nonbonded atomic interactions. *Protein Sci.* 2, 1511–1519 (1993).
- [56].Wiederstein, M. & Sippl, M. J. ProSA-web: Interactive web service for the recognition of errors in three-dimensional structures of proteins. *Nucleic Acids Res.* 35, 407–410 (2007).
- [57].Laskowski, R. A., MacArthur, M. W., Moss, D. S. & Thornton, J. M. PROCHECK: a program to check the stereochemical quality of protein structures. *J. Appl. Crystallogr.* 26, 283–291 (1993).
- [58].Trott, O. & Olson, A. Software News and Updates Gabedit — A Graphical User Interface for Computational Chemistry Softwares. *J. Comput. Chem.* 32, 174–182 (2012).
- [59].Eberhardt, J., Santos-Martins, D., Tillack, A. F. & Forli, S. AutoDock Vina 1.2.0: New Docking Methods, Expanded Force Field, and Python Bindings. *J. Chem. Inf. Model.* 61, 3891–3898 (2021).
- [60].Kim, S. et al. PubChem in 2021: New data content and improved web interfaces. *Nucleic Acids Res.* 49, D1388–D1395 (2021).
- [61].Madej, M., Kurowska, N. & Strzalka-Mroziak, B. Polymeric Nanoparticles—Tools in a Drug Delivery System in Selected Cancer Therapies. *Applied Sciences (Switzerland)* 12, (2022).
- [62].Perumal, S. Polymer Nanoparticles Synthesis and Applications. *Polymers (Basel)*. 14, 5449 (2022).
- [63].Zielinska, A. et al. Polymeric Nanoparticles: Production, Characterization, Toxicology and Ecotoxicology. *Molecules* 25, (2020).
- [64].Ramalho, M. J. & Pereira, M. C. Preparation and Characterization of Polymeric Nanoparticles: An Interdisciplinary Experiment. *J. Chem. Educ.* 93, 1446–1451 (2016).
- [65].Muhamad, I. I., Selvakumaran, S., Asmak, N. & Lazim, M. Designing Polymeric Nanoparticles for Targeted Drug Delivery System.
- [66].Yao, F. & Weiyuan, J. Drug Release Kinetics and Transport Mechanisms of Non- degradable and Degradable Polymeric Delivery Systems. *Expert Opin Drug Deliv.* 7, 429–444. (2010).
- [67].Vieira, A. C., Guedes, R. M. & Marques, A. T. Development of ligament tissue biodegradable devices: A review. *J. Biomech.* 42, 2421–2430 (2009).
- [68].Sabino, M. A., Morales, D., Ronca, G. & Feijoo, L. Estudio de la Degradación Hidrolítica de un Copolíme-

- ro Biodegradable. *Acta Científica Venez.* 54, 18–27 (2003).
- [69]. Scaffaro, R., Lopresti, F. & Botta, L. Preparation, characterization and hydrolytic degradation of PLA/PCL co-mingled nanofibrous mats prepared via dual-jet electrospinning. *Eur. Polym. J.* 96, 266–277 (2017).
- [70]. Elsayy, M. A., Kim, K. H., Park, J. W. & Deep, A. Hydrolytic degradation of polylactic acid (PLA) and its composites. *Renew. Sustain. Energy Rev.* 79, 1346–1352 (2017).
- [71]. Zaaba, N. F. & Jaafar, M. A review on degradation mechanisms of polylactic acid: Hydrolytic, photodegradative, microbial, and enzymatic degradation. *Polym. Eng. Sci.* 60, 2061–2075 (2020).
- [72]. Hurtado, L. & Sabino, M. Estudio del Proceso de Liberación de una Chalcona presente en Estructuras para Aplicaciones Biomédicas. (Universidad Simón Bolívar, 2018).
- [73]. Törmälä, P., Pohjonen, T. & Rokkanen, P. Bioabsorbable polymers: Materials technology and surgical applications. *Proc. Inst. Mech. Eng. Part H J. Eng. Med.* 212, 101–111 (1998).
- [74]. WHO. Cancer. (2022). <https://www.who.int/news-room/fact-sheets/detail/cancer> [accessed 7 October 2024].
- [75]. Castells, A., Rodríguez-Moranta, F. & Soriano, A. Implicación de ciclooxigenasa 2 en el cáncer : utilidad de los coxib. *Rev Esp Reum.* 30, 386–92 (2003).
- [76]. Dannenberg, A. et al. Cyclo-oxygenase 2: A pharmacological target for the prevention of cancer. *Lancet Oncol* 2, 544–551 (2001).
- [77]. Ruilope, L. & Coca, A. Inhibidores selectivos de la ciclooxigenasa-2 (Coxibs) y morbilidad cardiovascular. *Med. Clin. (Barc.)* 118, 219–221 (2022).
- [78]. Tsujii, M., Kawano, S. & Dubois, R. N. Cyclooxygenase-2 expression in human colon cancer cells increases metastatic potential. *Proc. Natl. Acad. Sci. U. S. A.* 94, 3336–3340 (1997).
- [79]. Ballón, W. & Grados, R. Acomplamiento molecular: criterios prácticos para la selección de ligandos biológicamente activos e identificación de nuevos blancos terapéuticos. *Rev.Cs.Farm. y Bioq* 7, 1–18 (2019).
- [80]. Stanzione, F., Giangreco, I. & Cole, J. Use of molecular docking computational tools in drug discovery. *Prog. Med. Chem.* 60, 273–343 (2021).
- [81]. Ikram, M. et al. Synthesis, molecular docking evaluation for LOX and COX-2 inhibition and determination of in-vivo analgesic potentials of aurone derivatives. *Heliyon* 10, e29658 (2024).
- [82]. Daina, A., Michielin, O. & Zoete, V. SwissADME: A free web tool to evaluate pharmacokinetics, drug-likeness and medicinal chemistry friendliness of small molecules. *Sci. Rep.* 7, 1–13 (2017).